Scientific Research Publishing

International Journal of Astronomy and Astrophysics, 2025, 15(3), 264-281
https://www.scirp.org/journal/ijaa
ISSN Online: 2161-4725
ISSN Print: 2161-4717

The Warm Dark Matter plus Baryon Linear Power Spectrum

Bruce Hoeneisen

Universidad San Francisco de Quito, Quito, Ecuador
Email: bhoeneisen@usfq.edu.ec

How to cite this paper: Hoeneisen, B. (2025) The Warm Dark Matter plus Baryon Linear Power Spectrum. *International Journal of Astronomy and Astrophysics*, **15**, 264-281.
https://doi.org/10.4236/ijaa.2025.153017

Received: May 21, 2025
Accepted: August 5, 2025
Published: August 8, 2025

Abstract

We study linear density perturbations in an extension of Newtonian cosmology. The extension includes warm dark matter and baryons. The effect of the warm dark matter particle thermal velocity is to prevent short wavelength perturbations from growing. We obtain the linear power spectrum relative to cold dark matter, prior to galaxy formation, for warm dark matter with a Maxwell or Bose-Einstein thermal velocity distribution. This prediction can be tested with precision weak gravitational lensing observations of the cosmic microwave background radiation.

Keywords

Warm Dark Matter, Galaxy, Power Spectrum

1. Introduction

We try to understand dark matter with galaxy observations. From studies of publicly available galaxy data we have obtained several insights, some of which are contrary to common belief, and most of which are surely not original. Here is a list:

1) Dwarf and spiral galaxy rotation curves, and elliptical galaxy density runs, are (generally) well described by isothermal hydrostatic equations of self-gravitating gases of warm dark matter and baryons [1] [2]. These equations break down for cold dark matter, suggesting that dark matter is indeed warm.

2) Fits to these galaxy rotation curves allow a measurement of the warm dark matter adiabatic invariant $v_{hrms}(1) = v_{hrms}(a)a = 406 \pm 69$ m/s, that we interpret to be of cosmological origin, with far-reaching consequences. $v_{hrms}(a)$ is the root-mean-square thermal velocity of non-relativistic dark matter particles at expansion parameter a. Arguments in favor of, and against, the cosmological interpretation of $v_{hrms}(1)$ can be found in [1] and [3], so we need more observa-

tions to settle the issue.

3) My prejudice is that dark matter is ultra-relativistic in the remote past, as everything else. Hence, it is convenient to add one more parameter to the six-parameter ΛCDM cosmology, namely $a_{h\mathrm{NR}} \equiv v_{h\mathrm{rms}}(1)/c$.

4) The solution of the hydrostatic equations is the cored isothermal sphere of warm dark matter plus baryons. This cored isothermal sphere is the building block for understanding galaxies.

5) If the core is dominated by dark matter, as in some dwarf galaxies, then the radius of the core is of cosmological origin [4].

6) The kinetic plus potential energy of the warm dark matter particles in the cored isothermal sphere follows the Maxwell-Boltzmann distribution, with a temperature independent of the radial coordinate r [2] [5].

7) Cored isothermal spheres in an expanding universe grow faster than the separation between galaxies [4] [6]. As time goes on, galaxy halos overlap, some galaxies coalesce, and others lose matter to neighbors. This allows an understanding of the bottom-up and top-down hierarchical evolution of galaxies.

8) Due to the expansion of the universe, the galaxy halos already grow in thermal equilibrium, without the need for relaxation, resulting in extended flat rotation curves [4] [6].

9) The isothermal sphere in an expanding universe has no "virial mass" [4] [6].

10) The formation of galaxies is well described by hydrodynamical equations of self-gravitating warm dark matter and baryons [2].

11) The Press-Schechter formalism describes well the distributions of the stellar masses and ultra-violet luminosities of galaxies in a wide range of redshifts [7], so long as a "tail" is added to the warm dark matter cut-off function with the assumed form:

$$\tau^2(q) \approx \begin{cases} \exp\left(-\dfrac{q^2}{q_{\mathrm{fs}}^2}\right) & \text{if } q < q_{\mathrm{fs}} \\ \exp\left(-\dfrac{q^n}{q_{\mathrm{fs}}^n}\right) & \text{if } q \geq q_{\mathrm{fs}} \end{cases} \tag{1}$$

Agreement is obtained for n in the range 0.5 to 1.1 [8]. Here $\tau^2(q)$ is the ratio of warm-to-cold density perturbation power spectrums $\tau^2(q) \equiv P_{\mathrm{WDM}}(q)/P_{\mathrm{CDM}}(q)$ at the time of galaxy formation, including the non-linear regeneration of structure. The origin of the "tail", if it exists, is not currently understood, and is one of the motivations of the present study.

12) The measured adiabatic invariant $v_{h\mathrm{rms}}(1)$ agrees with dark matter particles coupled to the Higgs boson, with mass $m_h \approx 150$ eV, spin zero, and temperature $T_S(a) \approx 0.343 \cdot T_\gamma(a)$ after e^+e^- annihilation while ultra-relativistic [1]. These dark matter particles become non-relativistic at a characteristic expansion parameter $a_{h\mathrm{NR}} = v_{h\mathrm{rms}}(1)/c \approx 1.4 \times 10^{-6}$. Dirac or Majorana spin-$\frac{1}{2}$, and vector spin-1, dark matter particles are disfavored by more than 5σ [1]. If Nature missed this

opportunity, then the measured $v_{hrms}(1)$ is an unlikely coincidence.

13) The dark matter particle mass $m_h \approx 150$ eV is in disagreement with many published limits. However, these disagreements are not final [3].

14) With the measured warm dark matter properties, we have updated the "New Minimal Standard Model" [9].

15) The hydrodynamical equations describe the first order perturbations of warm dark matter plus baryon densities, including the Jeans-like wavenumber that divides growing from decaying modes.

All of the preceding items have been derived from the set of hydrodynamical equations presented in Section 2 below, and have been published, except item 15. The purpose of the present article is to obtain the derivation corresponding to item 15, and predict the linear $\tau^2(q)$ for warm dark matter plus baryons, so that the interpretation of $v_{hrms}(1)$ can be tested with future observations. In particular, do baryons give $\tau^2(q)$ a significant tail?

2. The Hydrodynamical Equations

Notation: $a(t)$ is the expansion parameter of the universe, normalized to $a(t_0)=1$ at the present time t_0. t is the age of the universe. $\boldsymbol{X}(t)$ is the proper Euclidean coordinate, and $\boldsymbol{x}(t)=\boldsymbol{X}(t)/a(t)$ is the comoving coordinate. $\boldsymbol{q}$ is the comoving wavevector, and $\boldsymbol{q}/a(t)$ is the proper wavevector.
$\boldsymbol{v}(\boldsymbol{X},t)=\mathrm{d}\boldsymbol{X}(t)/\mathrm{d}t$ is the gas velocity, and $v_{\mathrm{rms}}(\boldsymbol{X},t)$ is the particle 3-D thermal velocity relative to the gas rest frame. $\rho(\boldsymbol{X},t)$ is the density, and $\phi(\boldsymbol{X},t)$ is the Newtonian gravitational potential. The subindex 0 stands for "present day" value. We use the subindex h for warm dark matter, and the subindex b for baryons. Alternatively, the subindices h and b may stand for two warm dark matter components. Generalizing to more components is straightforward. In cosmology, "baryons" generally refer to the non-relativistic matter, excluding dark matter and neutrinos. We use the standard notation of [10].

This is the set of equations. They are a generalization of the equations of Newtonian cosmology, see Appendix F of Steven Weinberg's "Cosmology" [11]. The continuity equations are

$$\frac{\partial\rho_h}{\partial t}+\nabla\cdot\left(\boldsymbol{v}_h\rho_h\right)=0, \tag{2}$$

$$\frac{\partial\rho_b}{\partial t}+\nabla\cdot\left(\boldsymbol{v}_b\rho_b\right)=0, \tag{3}$$

the Euler equations are

$$\frac{\mathrm{d}\boldsymbol{v}_h}{\mathrm{d}t}=\frac{\partial\boldsymbol{v}_h}{\partial t}+\left(\boldsymbol{v}_h\cdot\nabla\right)\boldsymbol{v}_h=-\nabla\phi-\frac{1}{\rho_h}\nabla\left(\frac{1}{3}v_{hrms}^2\rho_h\right), \tag{4}$$

$$\frac{\mathrm{d}\boldsymbol{v}_b}{\mathrm{d}t}=\frac{\partial\boldsymbol{v}_b}{\partial t}+\left(\boldsymbol{v}_b\cdot\nabla\right)\boldsymbol{v}_b=-\nabla\phi-\frac{1}{\rho_b}\nabla\left(\frac{1}{3}v_{brms}^2\rho_b\right), \tag{5}$$

the Poisson equation is

$$\nabla^2\phi=4\pi G\left(\rho_h+\rho_b\right), \tag{6}$$

and the adiabatic invariant equations are

$$v_{hrms}(1)\rho_{h0}^{-1/3} = v_{hrms}(t)\rho_h^{-1/3}(t), \tag{7}$$

$$v_{brms}(1)\rho_{b0}^{-1/3} \approx v_{brms}(t)\rho_b^{-1/3}(t), \tag{8}$$

where $v_{hrms}(1) \equiv v_{hrms}(a=1) \equiv v_{hrms}(t_0)$. Equation (7) is valid for collisionless warm dark matter, or for collisional warm dark matter if collisions are elastic. Baryons have relaxation, *i.e.* excited states and inelastic collisions, so (8) is approximately valid only for some problems, and needs to be used with caution. Equation (5) becomes valid after baryons decouple from photons at $t = t_{dec}$.

3. Trying to Understand the Equations

Compared to the equations of Newtonian cosmology [11], we have added the equations for baryons, have added the last terms in (4) and (5), and have added the adiabatic invariant Equations (7) and (8).

Note that the velocity of a particle has two components: the fluid velocity $\boldsymbol{v}$, plus the random thermal velocity with respect to the local fluid rest frame (with 3D root-mean-square v_{rms}).

Integrating Equations (2) and (3) over a volume, we find that the change in the number of particles in the volume is equal to the number of particles that enter or exit through the surface of the volume. In other words, we only consider problems with no annihilation or creation of particles.

Equations (4) or (5), without the last terms, are Newton's equations, *i.e.* acceleration is equal to force per unit mass (in Newtonian language).

The terms with v_{hrms}^2 and v_{brms}^2 are non-trivial, specially for collisionless warm dark matter, and have far-reaching consequences. Removing these terms takes us from the warm dark matter scenario to the cold dark matter scenario, and prevents us from really understanding galaxies. If we remove these terms, our atmosphere would fall to the ground, and we would be unable to understand the "cored isothermal sphere" that is the building block of galaxies [2]. The last terms in (4) and (5), as well as Equations (7) and (8), are valid for collisional particles provided these collisions are elastic, or for collisionless particles provided there is no "relaxation", *i.e.* loosely speaking, $\boldsymbol{v}$ is single-valued. Note that warm dark matter "free-streaming" is already included in the hydrodynamical equations.

Remember that for a classical non-relativistic gas, with a Maxwell distribution of velocities, $\frac{1}{2}m\langle v^2\rangle = \frac{3}{2}kT$, and $P = nkT$. T, P and n are the temperature, pressure and particle number density of the gas. Here, k is the Boltzmann constant that corrects the units of T. For collisional particles, the last parenthesis in (5) is the gas pressure. Consider our atmosphere. Multiply the numerator and denominator of the last term in (5) by a horizontal surface S and a height dz. The result tells us that the difference in pressure from bottom to top times the surface per unit mass, *i.e.* the net force per unit mass, is what prevents that volume of atmosphere from falling.

However, this is not the best way to understand the last term in (4). This term is valid even for collisionless particles (if no relaxation). To try to explain this here would take us too far afield, so I refer the reader to the Feynman lectures on "The Exponential Atmosphere" [5]. Let me just say that studying these terms in detail would take us to Maxwell's velocity distribution, Boltzmann's distribution in "phase space" $\mathrm{d}^3\boldsymbol{x}\mathrm{d}^3\boldsymbol{p}$, and Liouville's theorem, as well as the adiabatic invariant Equations (7) and (8). All of these concepts are needed to understand the "cored isothermal sphere" and galaxies, see [2].

The Poisson equation tells us that the total matter is the source of gravity (in Newtonian language), and, as written, is valid only when the density of matter dominates. This Equation (6) couples warm dark matter with baryons.

Now consider the adiabatic invariant Equation (8), and a gas in an expanding vessel. The density decreases, and so do the velocities of the particles as they bounce off the receding walls of the vessel, as in (8). Alternatively, recall that, for a collisional noble gas, *i.e.* a gas with elastic collisions, $TV^{\gamma-1}$ is constant with $\gamma = 5/3$, which again obtains (8). The adiabatic invariant equations are also valid for collisionless gases. Consider gas in the expanding universe. Then $v \propto 1/a$ (prove it [2]) and $\rho \propto 1/a^3$, which obtains (8). This argument also works for a fluid with a divergent $\boldsymbol{v}$, provided there is no "relaxation". Loosely speaking, relaxation occurs when, at a given point, there is more than one fluid velocity $\boldsymbol{v}$. Relaxation may occur during the formation of a galaxy halo, or during halo collisions, or in general, during the bottom-up and top-down hierarchical evolution of the universe structure. In practice, we measure $v'_{h\mathrm{rms}}(1)$ with galaxy rotation curves [1], and obtain a distribution with a maximum/minimum ratio approximately 3. It is the lower bound of this distribution that we identify with the adiabatic invariant $v_{h\mathrm{rms}}(1)$ of cosmological origin [1], since, within uncertainties, it is the same for galaxies spanning 4 orders of magnitude of stellar mass or absolute luminosity! [1] The width of the distribution of $v'_{h\mathrm{rms}}(1)$ is interpreted to be due to relaxation that can only increase $v'_{h\mathrm{rms}}(1)$.

Consider the isothermal atmosphere. $v_{b\mathrm{rms}}$ is independent of altitude. According to (5), the density of the atmosphere decreases exponentially with altitude. On the other hand, the adiabatic invariant Equation (8) tells us that if density decreases, so does $v_{b\mathrm{rms}}$. How is this possible? Is there a contradiction? Let me point out a difference between these equations. The adiabatic invariant equation refers to a *given set of particles*. On the other hand, the average $v_{b\mathrm{rms}}$ in the last term of (4) is taken over *different sets of particles* at different altitudes: the average at the higher altitude is only over those particles at the lower altitude with v_z sufficiently large to reach the higher altitude. For a more detailed understanding, I again refer the reader to [2] and [5].

The adiabatic invariant Equations (7) and (8) should not be omitted: they are necessary for a solution. In a numerical integration, after updating the densities in a time step $\mathrm{d}t$, we need to update the root-mean-square velocities. In other words, to arrive at Equations (23) and (24) below, we need (7) and (8).

The best way to understand the seven equations in Section 2 is to re-derive all of the insights listed in the introduction. We now turn to item 15 of the introduction. The present approach is complementary to [12] and [13].

4. Newtonian Cosmology

We present the solution of Equations (2) to (8) for the universe dominated by the non-relativistic matter density, well within the horizon, after baryons decouple from photons, *i.e.* for $t > t_{\rm dec}$, up to linear perturbation terms. The derivation is a generalization of Appendix F of [11].

The unperturbed solution follows. The coordinate of a comoving object is $\boldsymbol{X}(t) = \left[a(t)/a(t_0)\right]\boldsymbol{X}(t_0)$ where $a(t)$ is the expansion parameter. Then $\mathrm{d}\boldsymbol{X}/\mathrm{d}t \equiv \boldsymbol{v} = H(t)\,\boldsymbol{X}(t)$ with $H = \dot{a}/a$. This is the Hubble law, and $H(t)$ is the Hubble parameter. The unperturbed densities and gravitational potential are $\bar{\rho}_h = \rho_{h0}/a^3$, $\bar{\rho}_b = \rho_{b0}/a^3$, and $\bar{\phi} = 2\pi G\left(\bar{\rho}_h + \bar{\rho}_b\right)X^2/3$. The evolution of $a(t)$ is

$$\dot{a}^2 + K = \frac{8}{3}\pi G\left(\bar{\rho}_h + \bar{\rho}_b\right)a^2. \tag{9}$$

This is the Friedmann equation for the case when the density is dominated by non-relativistic matter. Here we set the "curvature constant", or "total energy constant", $K = 0$.

To the unperturbed solution we add relatively small perturbations: $\rho_h = \bar{\rho}_h + \delta\rho_h$, $\rho_b = \bar{\rho}_b + \delta\rho_b$, $\boldsymbol{v}_h = \boldsymbol{v} + \delta\boldsymbol{v}_h$, $\boldsymbol{v}_b = \boldsymbol{v} + \delta\boldsymbol{v}_b$, and $\phi = \bar{\phi} + \delta\phi$. The next step is to write the terms in Equations (2) to (6) of first order in these perturbations:

$$\frac{\partial\delta\rho_h}{\partial t} + 3H\delta\rho_h + H\boldsymbol{X}\cdot\nabla\delta\rho_h + \bar{\rho}_h\nabla\cdot\delta\boldsymbol{v}_h = 0, \tag{10}$$

$$\frac{\partial\delta\rho_b}{\partial t} + 3H\delta\rho_b + H\boldsymbol{X}\cdot\nabla\delta\rho_b + \bar{\rho}_b\nabla\cdot\delta\boldsymbol{v}_b = 0, \tag{11}$$

$$\frac{\partial\delta\boldsymbol{v}_h}{\partial t} + H\boldsymbol{X}\cdot\nabla\delta\boldsymbol{v}_h + H\delta\boldsymbol{v}_h = -\nabla\delta\phi - \frac{1}{3\bar{\rho}_h}\nabla\left(v^2_{h\mathrm{rms}}(1)\frac{\rho_h^{5/3}}{\rho_{h0}^{2/3}}\right), \tag{12}$$

$$\frac{\partial\delta\boldsymbol{v}_b}{\partial t} + H\boldsymbol{X}\cdot\nabla\delta\boldsymbol{v}_b + H\delta\boldsymbol{v}_b = -\nabla\delta\phi - \frac{1}{3\bar{\rho}_b}\nabla\left(v^2_{b\mathrm{rms}}(1)\frac{\rho_b^{5/3}}{\rho_{b0}^{2/3}}\right), \tag{13}$$

$$\nabla^2\delta\phi = 4\pi G\left(\delta\rho_h + \delta\rho_b\right). \tag{14}$$

Now we perform a Fourier transform in the comoving coordinate:

$$\delta\rho_h(\boldsymbol{X},t) = \int \mathrm{d}^3q \exp\left(\frac{i\boldsymbol{q}\cdot\boldsymbol{X}}{a(t)}\right)\delta\rho_{\boldsymbol{q}h}(t), \tag{15}$$

$$\delta\rho_{\boldsymbol{q}h}(t) = \frac{1}{\left(2\pi a(t)\right)^3}\int \mathrm{d}^3X \exp\left(-\frac{i\boldsymbol{q}\cdot\boldsymbol{X}}{a(t)}\right)\delta\rho_h(\boldsymbol{X},t), \tag{16}$$

and similarly for the remaining perturbations. $\boldsymbol{X}$ and $\boldsymbol{q}/a(t)$ are the proper space coordinate and wavevector, while $\boldsymbol{X}/a(t)$ and $\boldsymbol{q}$ are the comoving

space coordinate and wavevector. The resulting equations, in comoving wavevector space $\boldsymbol{q}$, are

$$\frac{\mathrm{d}\delta\rho_{\boldsymbol{q}h}}{\mathrm{d}t}+3H\delta\rho_{\boldsymbol{q}h}+\frac{i}{a}\bar{\rho}_h\boldsymbol{q}\cdot\delta\boldsymbol{v}_{\boldsymbol{q}h}=0, \tag{17}$$

$$\frac{\mathrm{d}\delta\rho_{\boldsymbol{q}b}}{\mathrm{d}t}+3H\delta\rho_{\boldsymbol{q}b}+\frac{i}{a}\bar{\rho}_b\boldsymbol{q}\cdot\delta\boldsymbol{v}_{\boldsymbol{q}b}=0, \tag{18}$$

$$\frac{\mathrm{d}\delta\boldsymbol{v}_{\boldsymbol{q}h}}{\mathrm{d}t}+H\delta\boldsymbol{v}_{\boldsymbol{q}h}=-\frac{i}{a}\boldsymbol{q}\delta\phi_{\boldsymbol{q}}-\frac{5i}{9a^3}v_{h\mathrm{rms}}^2(1)\boldsymbol{q}\left(\frac{\delta\rho_{\boldsymbol{q}h}}{\bar{\rho}_h}\right), \tag{19}$$

$$\frac{\mathrm{d}\delta\boldsymbol{v}_{\boldsymbol{q}b}}{\mathrm{d}t}+H\delta\boldsymbol{v}_{\boldsymbol{q}b}=-\frac{i}{a}\boldsymbol{q}\delta\phi_{\boldsymbol{q}}-\frac{5i}{9a^3}v_{b\mathrm{rms}}^2(1)\boldsymbol{q}\left(\frac{\delta\rho_{\boldsymbol{q}b}}{\bar{\rho}_b}\right), \tag{20}$$

$$\boldsymbol{q}^2\delta\phi_{\boldsymbol{q}}=-4\pi Ga^2\left(\delta\rho_{\boldsymbol{q}h}+\delta\rho_{\boldsymbol{q}b}\right). \tag{21}$$

There are vector modes and scalar modes [11]. In vector modes, all scalar perturbations, including $\boldsymbol{q}\cdot\delta\boldsymbol{v}_{\boldsymbol{q}h}$ and $\boldsymbol{q}\cdot\delta\boldsymbol{v}_{\boldsymbol{q}b}$, vanish. Since these vector modes do not couple to gravity, they are decaying modes, with $\delta\boldsymbol{v}_{\boldsymbol{q}h}\propto 1/a$, and here we will ignore them. For scalar, *i.e.* compressional, modes we may write

$$\delta\boldsymbol{v}_{\boldsymbol{q}h}\equiv i\boldsymbol{q}\delta u_{\boldsymbol{q}h}\quad\text{and}\quad\delta\boldsymbol{v}_{\boldsymbol{q}b}\equiv i\boldsymbol{q}\delta u_{\boldsymbol{q}b}. \tag{22}$$

To eliminate $\delta u_{\boldsymbol{q}h}$ and $\delta u_{\boldsymbol{q}b}$ from the preceeding equations, we take the derivative of (17) with respect to t, replace $\mathrm{d}\delta u_{\boldsymbol{q}h}/\mathrm{d}t$ from (19), replace $\delta u_{\boldsymbol{q}h}$ from (17), and replace $\delta\phi_{\boldsymbol{q}}$ from (21). Simplyfing the notation with $\delta_{\boldsymbol{q}h}\equiv\delta\rho_{\boldsymbol{q}h}/\bar{\rho}_h$ and $\delta_{\boldsymbol{q}b}\equiv\delta\rho_{\boldsymbol{q}b}/\bar{\rho}_b$, we obtain

$$\frac{\mathrm{d}^2\delta_{\boldsymbol{q}h}}{\mathrm{d}t^2}+2H\frac{\mathrm{d}\delta_{\boldsymbol{q}h}}{\mathrm{d}t}=\frac{3H^2}{2}\left(\frac{\delta\rho_{\boldsymbol{q}h}+\delta\rho_{\boldsymbol{q}b}}{\bar{\rho}_h+\bar{\rho}_b}\right)-\frac{5}{9}\frac{\boldsymbol{q}^2}{a^4}v_{h\mathrm{rms}}^2(1)\delta_{\boldsymbol{q}h}, \tag{23}$$

$$\frac{\mathrm{d}^2\delta_{\boldsymbol{q}b}}{\mathrm{d}t^2}+2H\frac{\mathrm{d}\delta_{\boldsymbol{q}b}}{\mathrm{d}t}=\frac{3H^2}{2}\left(\frac{\delta\rho_{\boldsymbol{q}h}+\delta\rho_{\boldsymbol{q}b}}{\bar{\rho}_h+\bar{\rho}_b}\right)-\frac{5}{9}\frac{\boldsymbol{q}^2}{a^4}v_{h\mathrm{rms}}^2(1)\delta_{\boldsymbol{q}b}. \tag{24}$$

Solving (9) with $K=0$, $\bar{\rho}_b+\bar{\rho}_h=\Omega_m\rho_{\mathrm{crit}}/a^3$ and $\rho_{\mathrm{crit}}=3H_0^2/(8\pi G)$, obtains $H\equiv\dot{a}/a=H_0\sqrt{\Omega_m/a^3}=2/(3t)$. With the change of variable $\hat{t}\equiv t/t_{\mathrm{eq}}$, with

$$t_{\mathrm{eq}}\approx\frac{a_{\mathrm{eq}}^2}{2H_0\sqrt{\Omega_r}}\approx\frac{a_{\mathrm{eq}}^{3/2}}{2H_0\sqrt{\Omega_m}}, \tag{25}$$

we obtain

$$\begin{aligned}&\hat{t}^{4/3}\frac{\mathrm{d}^2\delta_{\boldsymbol{q}h}}{\mathrm{d}\hat{t}^2}+\frac{4}{3}\hat{t}^{1/3}\frac{\mathrm{d}\delta_{\boldsymbol{q}h}}{\mathrm{d}\hat{t}}\\&=\frac{2}{3\hat{t}^{2/3}}\frac{\delta_{\boldsymbol{q}h}\Omega_c+\delta_{\boldsymbol{q}b}\Omega_b}{\Omega_c+\Omega_b}\left(1-\frac{1}{\hat{t}^{2/3}}\frac{\boldsymbol{q}^2}{q_{Jh}^2(t_{\mathrm{eq}})}\frac{\delta_{\boldsymbol{q}h}(\Omega_c+\Omega_b)}{\delta_{\boldsymbol{q}h}\Omega_c+\delta_{\boldsymbol{q}b}\Omega_b}\right),\end{aligned} \tag{26}$$

$$\begin{aligned}&\hat{t}^{4/3}\frac{\mathrm{d}^2\delta_{\boldsymbol{q}b}}{\mathrm{d}\hat{t}^2}+\frac{4}{3}\hat{t}^{1/3}\frac{\mathrm{d}\delta_{\boldsymbol{q}b}}{\mathrm{d}\hat{t}}\\&=\frac{2}{3\hat{t}^{2/3}}\frac{\delta_{\boldsymbol{q}h}\Omega_c+\delta_{\boldsymbol{q}b}\Omega_b}{\Omega_c+\Omega_b}\left(1-\frac{1}{\hat{t}^{2/3}}\frac{\boldsymbol{q}^2}{q_{Jb}^2(t_{\mathrm{eq}})}\frac{\delta_{\boldsymbol{q}b}(\Omega_c+\Omega_b)}{\delta_{\boldsymbol{q}h}\Omega_c+\delta_{\boldsymbol{q}b}\Omega_b}\right),\end{aligned} \tag{27}$$

where

$$q_{Jh}\left(t_{\rm eq}\right)=1.22\sqrt{\frac{4\pi G\Omega_m\rho_{\rm crit}a_{\rm eq}}{v_{h\rm rms}^2\left(1\right)}}, \tag{28}$$

and similarly for $q_{Jb}\left(t_{\rm eq}\right)$. As an example, for $v_{h\rm rms}\left(1\right)=493$ m/s, $q_{Jh}\left(t_{\rm eq}\right)=2.0$ Mpc^{-1}.

Consider Equation (26). In the case of no baryons, and at low $\boldsymbol{q}^2$, we recover the well known equation of Newtonian cosmology [11]. The new features are the warm dark matter Jeans cut-off wavevector $q_{Jh}\left(t_{\rm eq}\right)$, and the addition of baryons that couple to the dark matter.

5. Solutions

We will solve Equations (26) and (27) from $t_{\rm eq}$ to a time $t_{\rm gal}$ before the formation of first galaxies, while the relative density perturbations are still linear. The baryon relative perturbations are allowed to start growing later, at decoupling at $t_{\rm dec}$.

Let us neglect baryons. At low comoving momenta $\boldsymbol{q}$, or for cold dark matter with very large $q_{Jb}\left(t_{\rm eq}\right)$, we can neglect the last term in (26). In this case the relative density perturbation $\delta\rho_{\boldsymbol{q}h}/\bar{\rho}_h$ for the scalar modes evolve in proportion to $t^{2/3}$ or t^{-1}. These are the well known growing and decaying scalar modes of Newtonian cosmology. At larger $\boldsymbol{q}^2$, the right hand side of (26) becomes negative, and the growing mode becomes a decaying mode. The transition wavevector at $t_{\rm eq}$ is $q_{Jh}\left(t_{\rm eq}\right)$. Note that, for $t>t_{\rm eq}$, $q_{Jh}\left(t\right)=q_{Jh}\left(t_{\rm eq}\right)\hat{t}^{1/3}=q_{Jh}\left(t_{\rm eq}\right)\sqrt{a/a_{\rm eq}}$ grows in proportion to $\sqrt{a}$, allowing non-linear re-generation of short wavelength density perturbations when first galaxy halos begin to form.

Let us now add baryons. Protons recombine with electrons to form neutral hydrogen at decoupling at time $t_{\rm dec}$. The temperature of these "baryons" at decoupling is $T_b=T_{\gamma 0}/a_{\rm dec}$. The comoving root-mean-square thermal velocity of baryons at $t_{\rm dec}$ is $v_{b\rm rms}\left(1\right)\approx\sqrt{3kT_b/m_N}\,a_{\rm dec}=8$ m/s. Due to residual ionization, the hydrogen and helium gas remains in thermal equilibrium with photons until redshift $z\approx 150$ [11]. At this redshift, $v_{b\rm rms}\left(1\right)\approx 21$ m/s. Thereafter, $T_b\propto a^{-2}$, so $v_{b\rm rms}\left(1\right)$ remains 21 m/s. So, after decoupling from the photons, baryons, *i.e.* mostly neutral hydrogen and helium atoms, behave as cold dark matter, *i.e.* $v_{b\rm rms}^2\left(1\right)\ll v_{h\rm rms}^2\left(1\right)$ for our scenario of interest. We therefore neglect the term with $q_{Jb}\left(t_{\rm eq}\right)$ in (27). We note that the proper sound speed of the hydrogen and helium gas is $v_s=\sqrt{5kT_b/\left(3\mu m_N\right)}$, with a mean molecular weight $\mu=1.22$ [11].

We present numerical solutions to the coupled Equations (26) and (27) in **Figure 1**. The horizontal axis is $\hat{t}\equiv t/t_{\rm eq}$, and extends up to the time corresponding to the formation of first galaxies, *i.e.* at an expansion parameter of order $a_{\rm gal}\equiv 1/21$. To guide the eye, we present, with a continuous black line, the cold dark matter solution $a/a_{\rm gal}=\left(t/t_{\rm gal}\right)^{2/3}$, normalized to 1 at $t_{\rm gal}$. The runs are defined by the Jeans suppression parameter $q/q_{Jh}\left(t_{\rm eq}\right)$ (see Equation (26)), as indicated in each figure. The top left figure with $q/q_{Jh}=0$ corresponds to cold

dark matter plus baryons. We set the initial $\delta_{qb}=0$, $\mathrm{d}\delta_{qh}/\mathrm{d}t=\mathrm{d}\delta_{qb}/\mathrm{d}t=0$, and the initial δ_{qh} so that the total relative matter density fluctuation $\delta\rho/\overline{\rho}$ matches the cold dark matter reference at t_{gal}.

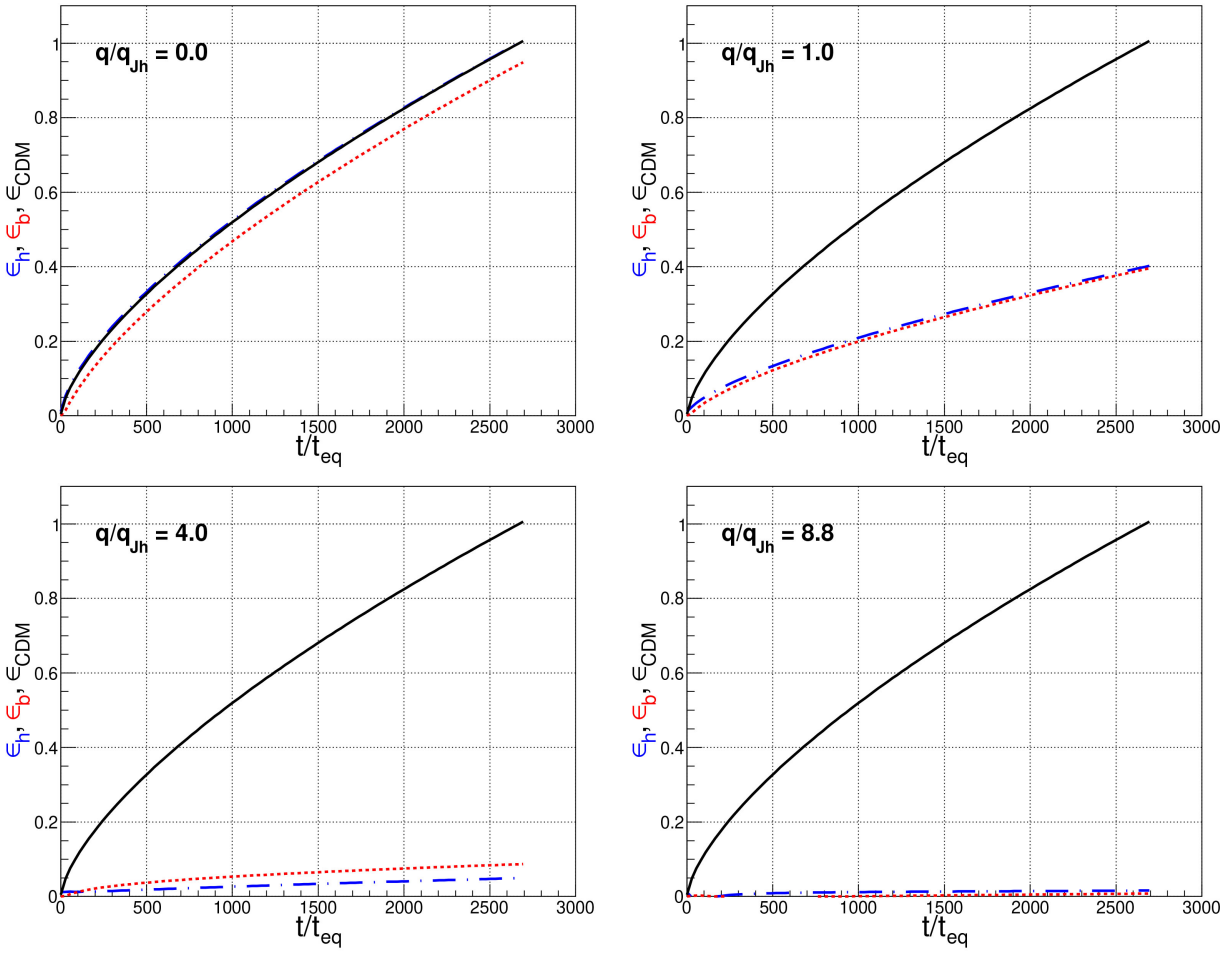

Figure 1. Relative density perturbations of warm dark matter $\delta_{qh}\equiv\delta\rho_{qh}/\overline{\rho}_h$ (dot-dashed blue), baryons $\delta_{qb}\equiv\delta\rho_{qb}/\overline{\rho}_b$ (dotted red) and cold dark matter δ_{CDM} for reference (continuous black), as a function of t/t_{eq} (normalized to cold dark matter =1 at $t_{\mathrm{gal}}/t_{\mathrm{eq}}$). t_{gal} corresponds to $a_{\mathrm{gal}}=1/21$. The warm dark matter Jeans suppression parameter $q/q_{Jh}(t_{\mathrm{eq}})$, is indicated in the legends.

6. Initial Conditions

We need initial conditions for δ_{qh} and $\mathrm{d}\delta_{qh}/\mathrm{d}t$ at t_{eq}, and δ_{qb} and $\mathrm{d}\delta_{qb}/\mathrm{d}t$ at t_{dec}. Since the equations of interest (26) and (27) are linear, we will normalize the results to the cold dark matter power spectrum at $a_{h\mathrm{NR}}=1/21$ (results are insensitive to the exact value chosen for $a_{h\mathrm{NR}}$, see the figures below).

Let us now consider the period $t_{h\mathrm{NR}}<t<t_{\mathrm{eq}}$ when the density of radiation dominates, and after warm dark matter becomes non-relativistic. Here we neglect δ_{qb}, as justified in Section 7. In this period baryons are coupled to the photons. For warm dark matter scalar modes, the hydrodynamical equation, obtained from (23) (but justified with General Relativity [11]) is

$$\frac{\mathrm{d}^2\delta_{\boldsymbol{q}h}}{\mathrm{d}t^2}+2H\frac{\mathrm{d}\delta_{\boldsymbol{q}h}}{\mathrm{d}t}=\frac{4\pi G\rho_{\mathrm{crit}}}{a^3}\delta_{\boldsymbol{q}h}\Omega_c-\frac{5}{9}\frac{\boldsymbol{q}^2}{a^4}v_{h\mathrm{rms}}^2(1)\delta_{\boldsymbol{q}h}, \tag{29}$$

with $H\equiv\dot{a}/a=H_0\sqrt{\Omega_r/a^4+\Omega_m/a^3}$. Equation (29) for cold dark matter, *i.e.* $v_{h\mathrm{rms}}(1)=0$, is the Mészáros equation, with the growing solution

$$\delta_{\boldsymbol{q}h}=1+\frac{3}{2}\frac{a}{a_{\mathrm{eq}}}. \tag{30}$$

So dark matter relative perturbations grow slowly within the horizon for $t<t_{\mathrm{eq}}$. The right-hand-side of (29) becomes zero at

$$q_{Jh}=1.34\sqrt{\frac{4\pi G\Omega_m\rho_{\mathrm{crit}}a}{v_{h\mathrm{rms}}^2(1)}}. \tag{31}$$

At $q>q_{Jh}$ the solution to (29) becomes oscillatory. For example, at early times $t\ll t_{\mathrm{eq}}$, the two solutions have the form $\delta'_{\boldsymbol{q}h}\propto\hat{t}^{-i\alpha}=\exp\left[-i\alpha\ln\left(\hat{t}\right)\right]$ with

$$\alpha^2=\frac{5\boldsymbol{q}^2v_{h\mathrm{rms}}^2(1)}{36H_0^2\Omega_r}. \tag{32}$$

In conclusion, the warm dark matter power spectrum at t_{eq}, is the same as the well known cold dark matter power spectrum at t_{eq}, except for warm dark matter free-streaming prior to $t_{h\mathrm{NR}}$.

For warm dark matter with comoving velocity v_h, the comoving free-streaming length from $t=0$ to $t=t_{h\mathrm{NR}}$, with expansion parameter $a_{h\mathrm{NR}}=v_h/c$, is

$$l_{\mathrm{fs}}(v_h)=\frac{v_h}{H_0\sqrt{\Omega_r}}. \tag{33}$$

Consider a cold dark matter density perturbation of the form e^{-iqz}, and compare it with a warm dark matter density perturbation obtained by displacing the particles a length $l_{\mathrm{fs}}(v_h)$ in random directions. The warm dark matter density perturbation becomes attenuated with respect to the cold dark matter perturbation by a factor

$$\tau_{\mathrm{fs}}(v_h,q)=\frac{\sin\left(ql_{\mathrm{fs}}(v_h)\right)}{ql_{\mathrm{fs}}(v_h)}. \tag{34}$$

Note that $\tau_{\mathrm{fs}}^2(v_h,q'_{\mathrm{fs}})\equiv 1/e$ at $q=q'_{\mathrm{fs}}=0.26\cdot 2\pi/l_{\mathrm{fs}}(v_h)$. This q'_{fs} is the same as q_{Jh} of (28), but with a coefficient 1.33 instead of 1.22. Since we will sample v_h sparsely, we will simply set $\tau_{\mathrm{fs}}(v_h,q)=0$ for $ql_{\mathrm{fs}}(v_h)>\pi$.

Our initial conditions are $\delta_{\boldsymbol{q}h}(v_h)\propto\tau_{\mathrm{fs}}(v_h,q)$ and $\mathrm{d}\delta_{\boldsymbol{q}h}/\mathrm{d}t=0$ at t_{eq}, and $\delta_{\boldsymbol{q}b}=0$ and $\mathrm{d}\delta_{\boldsymbol{q}b}/\mathrm{d}t=0$ at t_{dec}. We normalize $\delta_{\boldsymbol{q}h}(v_h)$ at t_{eq} so that the relative total matter density fluctuation matches cold dark matter at t_{gal}.

7. Baryons

The analytic expressions for $\delta_{\boldsymbol{q}h}$ and $\delta_{\boldsymbol{q}b}$ at time t_{dec}, for the cold dark matter scenario, can be found in [11]. They are the sum of a "slow" and a "fast" (oscillating) term. For warm dark matter, the slow components become multiplied by $\tau_{\mathrm{fs}}(v_h,q)$. Then

$$\frac{\delta_{qh}}{R_q^0} = -4.7\times10^2\,\tau_{\rm fs}(v_h,q) + 2.2\times10^{-4}\exp\left(-\int_0^t \Gamma\,dt\right)\cos\left(\int_0^t \frac{q\,dt}{a\sqrt{3(1+R)}}\right), \quad (35)$$

$$\frac{\delta_{qb}}{R_q^0} = -1.0\times10^{-5}\,\tau_{\rm fs}(v_h,q) - 2.7\exp\left(-\int_0^t \Gamma\,dt\right)\cos\left(\int_0^t \frac{q\,dt}{a\sqrt{3(1+R)}}\right), \quad (36)$$

at $q=1$ Mpc^{-1}. At $q=5$ Mpc^{-1} the coefficients are -4.2×10^2, 8.8×10^{-6}; -3.7×10^{-7} and -2.7, respectively. R_q^0 is the constant curvature perturbation outside the horizon. The oscillations are due to the sound speed $v_s = 1/\sqrt{3(1+R)}$ of the photon-baryon plasma, and the attenuation factor is due to the long neutrino mean free-path. $R \equiv 3\bar{\rho}_b/(4\bar{\rho}_\gamma)$.

In conclusion, the contribution of baryons to δ_{qb}/δ_{qh} at $t_{\rm eq}$ is negligible, *i.e.*

$$\approx -2.7\Omega_b/(-4.7\times10^2\,\Omega_c) = 0.001.$$

8. The Warm Dark Matter Cut-Off Factor $\tau^2(q)$

We consider two thermal velocity distributions: the Maxwell distribution, and the Bose-Einstein distribution with zero chemical potential. As an example, we assume a root-mean-square comoving thermal velocity $v_{h\rm rms}(1) = 493$ m/s, inspired by Table 4 of [1]. The final result (38) will not depend on this particular example. The interest in the Bose-Einstein and Maxwell velocity distributions is as follows. Dark matter particles may be bosons [1]. The ultra-relativistic dark matter may have the ultra-relativistic Bose-Einstein distribution. When, due to the expansion of the universe the dark matter becomes non-relativistic, it may acquire the non-relativistic Bose-Einstein distribution if collisionless, or may relax to the Maxwell distribution as explained in [14]. The cored isothermal sphere implies a Maxwell distribution. To cross-check one distribution with observations, it is necessary to have predictions for several distributions. So, both distributions are of observational interest.

In Table 1 and Table 2 we consider six warm dark matter thermal velocity bins. For each bin we obtain the root-mean-square velocity $v_{h\rm rms}$, the weight w for the Maxwell or Bose-Einstein distribution, the Jeans wavevector $q_{\rm Jh}(t_{\rm eq})$ from (28), and the comoving free-streaming length $l_{\rm fs}(v_h)$ from (33).

We consider six equations of the form (26) with relative perturbations δ_{qh1} to δ_{qh6}, corresponding to the six bins of v_h listed in Table 1 or Table 2. Instead of one Ω_c, we now have six $w_i\Omega_c$, with weights w_i corresponding to the Maxwell, or Bose-Einstein, distributions. We integrate numerically seven coupled equations: six of the form (26) for the warm dark matter in each velocity bin, and (27) for the baryons. The results are presented in Figure 2 and Figure 3.

This analysis obtains the predicted *linear* power spectrum warm dark matter cut-off factor $\tau^2(q) \equiv P_{\rm WDM}(q)/P_{\rm CDM}(q)$ at $t_{\rm gal}$, for the Maxwell and Bose-Einstein warm dark matter velocity distributions, see Figure 4. Note that if warm dark matter has a Bose-Einstein distribution, then there is a longer tail due to the excess of particles with low v_h that act as cold dark matter.

Table 1. For each warm dark matter thermal velocity bin we obtain the root-mean-square velocity v_{hrms} and weight w for a Maxwell distribution with total root-mean-square velocity 493 m/s. Also presented is the corresponding Jeans wavevector $q_{\mathrm{Jh}}(t_{\mathrm{eq}})$, and comoving free-streaming length $l_{\mathrm{fs}}(v_h)$ from $t=0$ to $t_{h\mathrm{NR}}(v_h)$.

$v_{h\min}$	$v_{h\max}$	v_{hrms}	$100w$	$q_{\mathrm{Jh}}(t_{\mathrm{eq}})$	$l_{\mathrm{fs}}(v_h)$
[m/s]	[m/s]	[m/s]		[Mpc^{-1}]	[Mpc]
0	75	58	0.48	16.70	0.090
75	175	139	5.05	6.96	0.217
175	375	293	31.57	3.30	0.457
375	625	494	44.37	1.96	0.772
625	875	721	16.14	1.34	1.126
875	∞	970	2.39	1.00	1.514

Table 2. For each warm dark matter thermal velocity bin we obtain the root-mean-square velociy v_{hrms} and weight w for a Bose-Einstein distribution, with zero chemical potential, with total root-mean-square velocity 493 m/s. Also presented is the corresponding Jeans wavevector $q_{\mathrm{Jh}}(t_{\mathrm{eq}})$, and comoving free-streaming length $l_{\mathrm{fs}}(v_h)$ from $t=0$ to $t_{h\mathrm{NR}}(v_h)$.

$v_{h\min}$	$v_{h\max}$	v_{hrms}	$100w$	$q_{\mathrm{Jh}}(t_{\mathrm{eq}})$	$l_{\mathrm{fs}}(v_h)$
[m/s]	[m/s]	[m/s]		[Mpc^{-1}]	[Mpc]
0	75	43	11.50	22.39	0.067
75	175	128	14.98	7.57	0.200
175	375	278	27.09	3.48	0.434
375	625	496	25.13	1.95	0.774
625	875	738	13.99	1.31	1.151
875	∞	1056	7.31	0.92	1.648

For predictions with the Press-Schechter formalism it is convenient to have an analytic approximation to $\tau^2(q)$. For the Maxwell distribution, we may simply take $\tau^2(q)=\exp\left(-q^2/q_{\mathrm{fs}}^2\right)$ with $q_{\mathrm{fs}}=1.41$ Mpc^{-1}, see **Figure 4**. For the Bose-Einstein distribution, $\tau^2(q)$ has the form

$$\tau^2(q)=\begin{cases}\exp\left(-\dfrac{q^2}{q_{\mathrm{fs}}^2}\right) & \text{if } q\le aq_{\mathrm{fs}},\\ \exp\left(1-a^2-\dfrac{q^n}{(a\cdot q_{\mathrm{fs}})^n}\right)+b & \text{if } q>aq_{\mathrm{fs}},\end{cases} \tag{37}$$

with $q_{\mathrm{fs}}=1.45$ Mpc^{-1}, $a=1.4$, $b=0.0006$ and $n=1.41$. Equation (26), and the initial conditions, depend on the combination $qv_{hrms}(1)$. Therefore, the horizontal axis q of **Figure 4** may be rescaled to other $v_{hrms}(1)$ different from 493 m/s. For example, for the Maxwell distribution,

$$q_{\mathrm{fs}}\left(t_{\mathrm{gal}}\right)=1.41\,\mathrm{Mpc}^{-1}\frac{493\ \mathrm{m/s}}{v_{h\mathrm{rms}}\left(1\right)}=0.88\sqrt{\frac{4\pi G\Omega_m\rho_{\mathrm{crit}}a_{\mathrm{eq}}}{v_{h\mathrm{rms}}^2\left(1\right)}}. \tag{38}$$

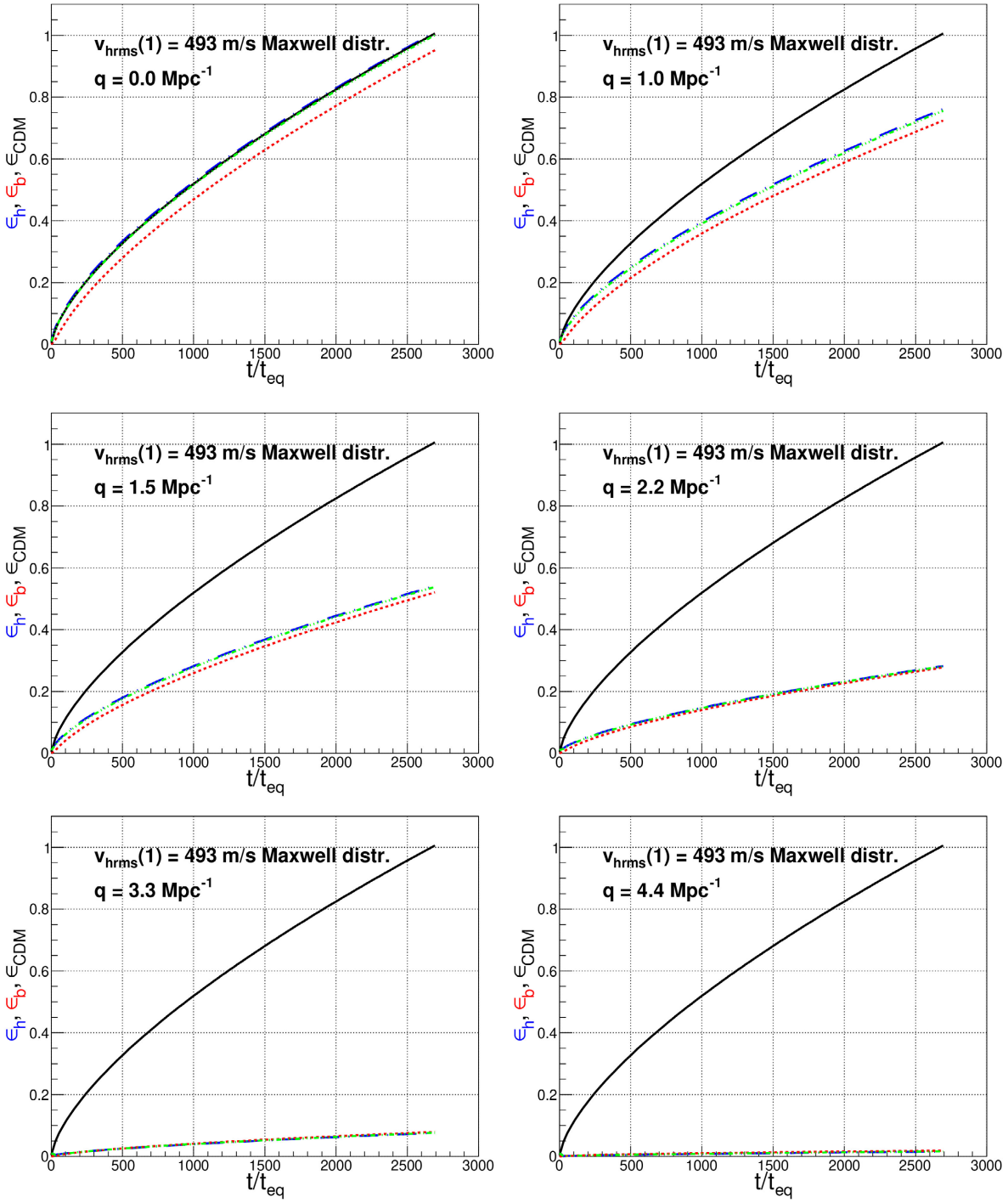

Figure 2. Relative density perturbations of warm dark matter $\delta\rho_{qh}/\overline{\rho}_h$ (dot-dashed blue), baryons $\delta\rho_{qb}/\overline{\rho}_b$ (dotted red), total $\left(\delta\rho_{qh}+\delta\rho_{qb}\right)/\left(\overline{\rho}_h+\overline{\rho}_b\right)$ (dashed-triple-dot green), and cold dark matter for reference (continuous black), as a function of t/t_{eq} (normalized to cold dark matter = 1 at $t_{\mathrm{gal}}/t_{\mathrm{eq}}$). t_{gal} corresponds to $a_{\mathrm{gal}}=1/21$. The wavevector q is indicated on each figure. The warm dark matter has a Maxwell velocity distribution with $v_{h\mathrm{rms}}\left(1\right)=493$ m/s.

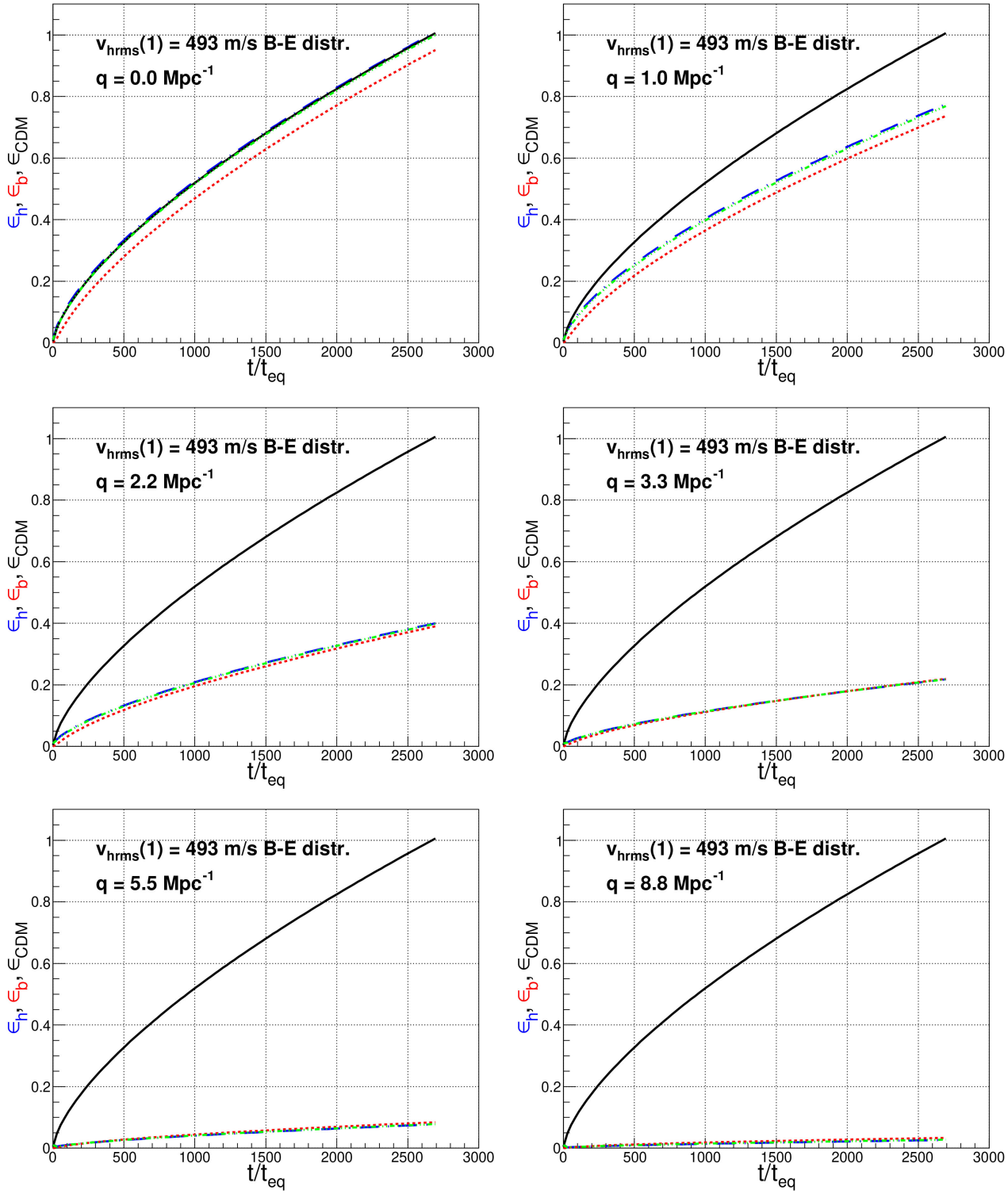

Figure 3. Same as **Figure 2**, but for a Bose-Einstein velocity distribution with zero chemical potential, with $v_{hrms}(1) = 493$ m/s.

We note that with $v_{hrms}(1) = 493$ m/s we obtain the values of $\tau^2(q)$ that fit the observed stellar mass and ultra-violet luminosity distributions in a wide redshift range [7], suggesting that $v_{hrms}(1)$ is indeed of order 493 m/s. An example

is presented in Figure 5. We do not have the resolution needed to distinguish the Maxwell from the Bose-Einstein distributions.

A measurement of the *linear* comoving power spectrum of density perturbations $P(q)$, prior to the formation of the first galaxies, will be able to obtain $v_{hrms}(1)$, and perhaps distinguish between the Maxwell and Bose-Einstein distributions. A compilation of measurements of the power spectrum $P(q)$ can be found in [15]. The Planck mission is sensitive to the linear power spectrum prior to galaxy formation, and reaches $q \approx 0.4$ Mpc^{-1}. Measurement of the linear power spectrum, up to $q \approx 20$ Mpc^{-1}, will become possible with high resolution weak gravitational lensing of the cosmic microwave background radiation (CMB) [16].

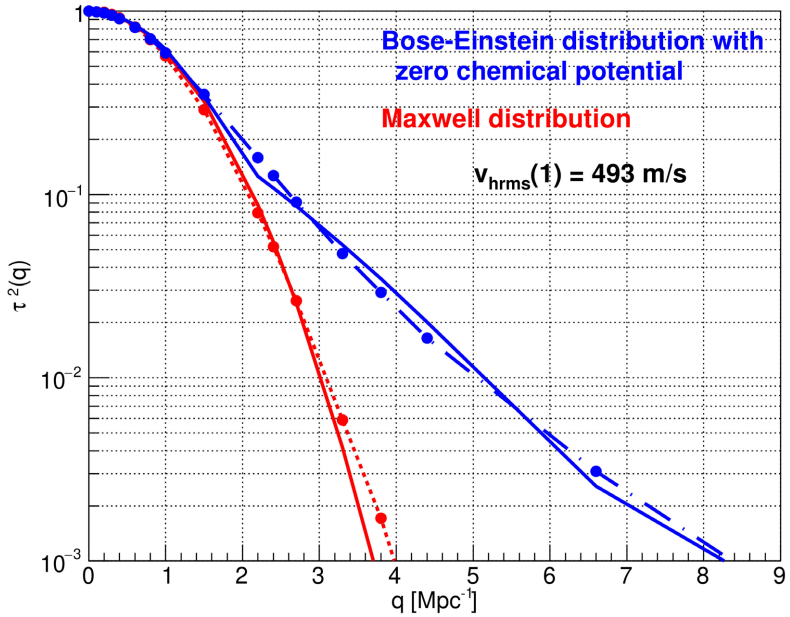

Figure 4. Warm dark matter plus baryon power spectrum cut-off factor $\tau^2(q)$, relative to cold dark matter at $a_{gal} = 1/21$, as a function of comoving wavevector q, for dark matter thermal velocities with a Maxwell distribution (red) or Bose-Einstein distribution with zero chemical potential (blue), with $v_{hrms} = 493$ m/s. Continuous lines in red or blue are analytic approximations described in the text.

Let us compare (38) (at t_{gal}) with Figure 5 of [12] (at t_{eq}) for $\tau^2(q_{fs}) \equiv 1/e$:

$$q_{fs}(t_{eq}) = 1.03\sqrt{\frac{4\pi G\Omega_m \rho_{crit} a_{eq}}{v_{hrms}^2(1)}}. \tag{39}$$

We note that the derivations of (38) and (39) are very different. Also noteworthy is a comparison of (38) with (28). A numerical calculation of $\tau^2(q)$ with CMBFAST or CAMB is presented in [17].

The effect of baryons can be illustrated as follows. For the Maxwell distribution at $q/q_{fs}(t_{eq}) = 2.2$ Mpc^{-1}, $\tau(q) = 0.361$ with baryons, and 0.291 without baryons.

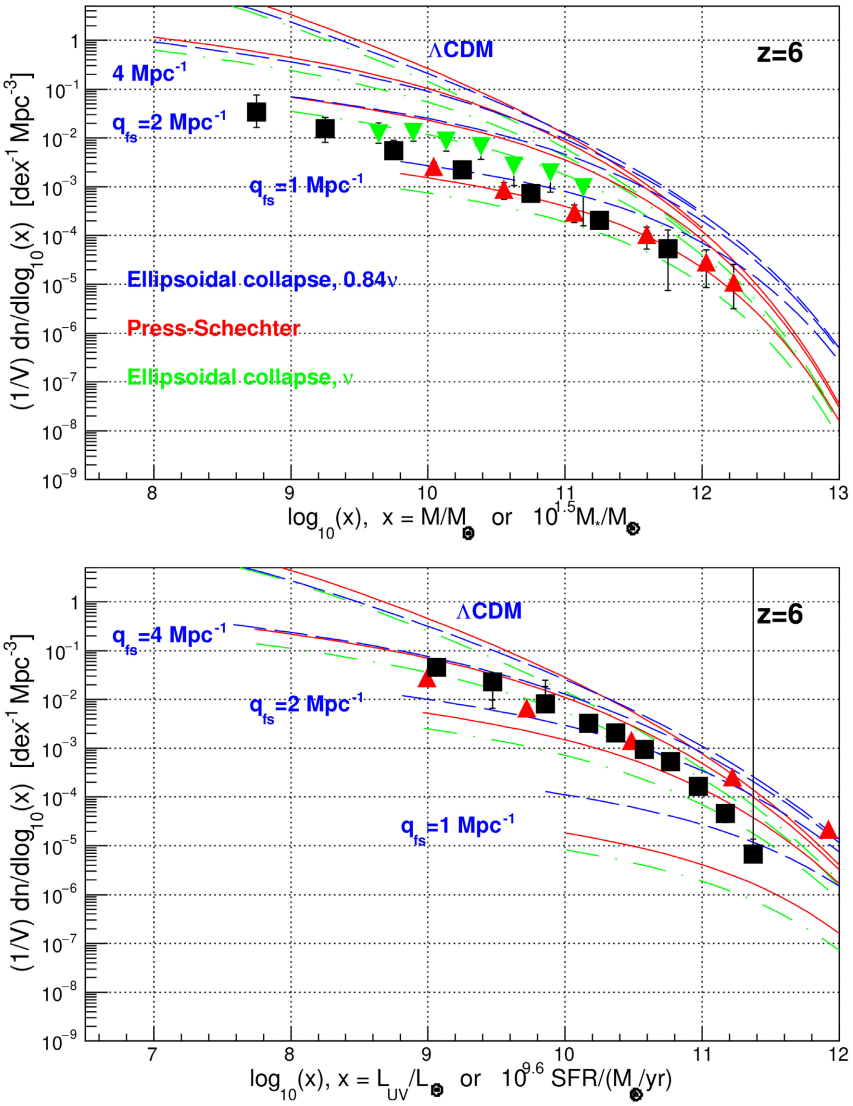

Figure 5. Comparison of predicted and observed distributions of $M/M_\odot = 10^{1.5}\, M_*/M_\odot$ (top panel) and $L_{UV}/L_\odot = 10^{9.6}\,\mathrm{SFR}/(M_\odot/\mathrm{yr})$ (bottom panel) for redshift $z = 6$. Data are from the Hubble Space Telescope (stellar mass M_* from [18] and ultra-violet luminosity L_{UV} from [19]) (black squares), from the continuity equation [20] (red triangles), and from the James Webb Space Telescope (green triangles) [21]. The predictions have $\tau^2(q) = \exp\left(-q^2/q_{\mathrm{fs}}^2\right)$ with q_{fs} as shown in the figure, corresponding to the Maxwell distribution. For full details, see [7]. $v_{hrms}(1) = 493\ \mathrm{m/s} \times 1.41\ \mathrm{Mpc}^{-1}/q_{\mathrm{fs}}$.

9. Conclusion

Hydrodynamical equations of warm dark matter and baryons allow an understanding of galaxy halos, galaxy rotation curves, stellar mass distributions, ultra-violet luminosity distributions, galaxy formation, and the hierarchical evolution of galaxies. These equations also describe the formation of structure in the expanding universe. Linear relative density perturbations are described by the coupled Equations (26) and (27). Solving these equations we have obtained predic-

tions of the linear power spectrum of relative density perturbations for two cases of interest: warm dark matter with a Maxwell or Bose-Einstein distribution of velocities. The predicted power spectrum may be tested with high precision weak gravitational lensing of the cosmic microwave background radiation [16].

Acknowledgements

I thank Karsten Müller for his early interest in this work and for many useful discussions.

Conflicts of Interest

The author declares no conflicts of interest regarding the publication of this paper.

References

[1] Hoeneisen, B. (2024) Measurements of the Dark Matter Mass, Temperature and Spin. *International Journal of Astronomy and Astrophysics*, **14**, 184-202. https://doi.org/10.4236/ijaa.2024.143012

[2] Hoeneisen, B. (2023) Understanding the Formation of Galaxies with Warm Dark Matter. *Journal of Modern Physics*, **14**, 1741-1754. https://doi.org/10.4236/jmp.2023.1413103

[3] Hoeneisen, B. (2025) Discrepancies between Limits and Measurements of Warm Dark Matter Properties. *International Journal of Astronomy and Astrophysics*, **15**, 65-79. https://doi.org/10.4236/ijaa.2025.152005

[4] Hoeneisen, B. (2025) Why Do Galaxies Have Extended Flat Rotation Curves? *International Journal of Astronomy and Astrophysics*, **15**, 1-10. https://doi.org/10.4236/ijaa.2025.151001

[5] Feynman, R.P., Leighton, R.B. and Sands, M. (1965) The Feynman Lectures on Physics. Addison-Wesley Publishing Company.

[6] Mistele, T., McGaugh, S., Lelli, F., Schombert, J. and Li, P. (2024) Indefinitely Flat Circular Velocities and the Baryonic Tully-Fisher Relation from Weak Lensing. arXiv: 2406.09685.

[7] Hoeneisen, B. (2024) Are James Webb Space Telescope Observations Consistent with Warm Dark Matter? *International Journal of Astronomy and Astrophysics*, **14**, 45-60. https://doi.org/10.4236/ijaa.2024.141003

[8] Hoeneisen, B. (2022) Measurement of the Dark Matter Velocity Dispersion with Galaxy Stellar Masses, UV Luminosities, and Reionization. *International Journal of Astronomy and Astrophysics*, **12**, 258-272. https://doi.org/10.4236/ijaa.2022.123015

[9] Hoeneisen, B. (2025) Update to the "New Minimal Standard Model". *International Journal of Astronomy and Astrophysics*, **15**, 43-63. https://doi.org/10.4236/ijaa.2025.151004

[10] Navas, S., *et al.* (2024) Review of Particle Physics. *Physical Review D*, **110**, Article ID: 030001.

[11] Weinberg, S. (2008) Cosmology. Oxford University Press.

[12] Boyanovsky, D., de Vega, H.J. and Sanchez, N.G. (2008) Dark Matter Transfer Function: Free Streaming, Particle Statistics, and Memory of Gravitational Clustering. *Physical Review D*, **78**, Article ID: 063546. https://doi.org/10.1103/physrevd.78.063546

[13] Boyanovsky, D. (2007) Free Streaming in Mixed Dark Matter. arXiv: 0711.0470.

[14] Paduroiu, S., Revaz, Y. and Pfenniger, D. (2015) Structure Formation in Warm Dark Matter Cosmologies Top-Bottom Upside-Down. arXiv: 1506.03789.

[15] Chabanier, S., Millea, M. and Palanque-Delabrouille, N. (2019) Matter Power Spectrum: From Ly A Forest to CMB Scales. *Monthly Notices of the Royal Astronomical Society*, **489**, 2247-2253. https://doi.org/10.1093/mnras/stz2310

[16] MacInnis, A. and Sehgal, N. (2024) CMB-HD as a Probe of Dark Matter on Sub-Galactic Scales. arXiv: 2405.12220.

[17] Viel, M., Lesgourgues, J., Haehnelt, M.G., Matarrese, S. and Riotto, A. (2005) Constraining Warm Dark Matter Candidates Including Sterile Neutrinos and Light Gravitinos with WMAP and the Lyman-α Forest. *Physical Review D*, **71**, Article ID: 063534. https://doi.org/10.1103/physrevd.71.063534

[18] Song, M., Finkelstein, S.L., Ashby, M.L.N., Grazian, A., Lu, Y., Papovich, C., *et al.* (2016) The Evolution of the Galaxy Stellar Mass Function at $z = 4 - 8$: A Steepening Low-Mass-End Slope with Increasing Redshift. *The Astrophysical Journal*, **825**, Article 5. https://doi.org/10.3847/0004-637x/825/1/5

[19] Bouwens, R.J., *et al.* (2021) New Determinations of the Luminosity Functions from $z \approx 9$ to $z \approx 2$ show Remarkable Consistency with Halo Growth and a Constant Star Formation Efficiency. arXiv: 2102.07775v1. https://arxiv.org/pdf/2102.07775.pdf

[20] Lapi, A., Mancuso, C., Bressan, A. and Danese, L. (2017) Stellar Mass Function of Active and Quiescent Galaxies via the Continuity Equation. *The Astrophysical Journal*, **847**, Article 13. https://doi.org/10.3847/1538-4357/aa88c9

[21] Navarro-Carrera, R., Rinaldi, P., Caputi, K.I., Iani, E., Kokorev, V. and van Mierlo, S. (2023) Constraints on the Faint End of the Galaxy Stellar Mass Function at $z \approx 4 - 8$ from Deep JWST Data. arXiv: 2305.16141.